

Uranium Series Disequilibrium and High Thorium and Radium Enrichments in Karst Formations

H. R. VON GUNTEN,^{*,†}
H. SURBECK,[‡] AND E. RÖSSLER[†]

Paul Scherrer Institut, CH-5232 Villigen PSI, Switzerland, and
Federal Office of Public Health, Radioactivity Survey Section
(SUEr), Chemin du Musée, CH-1700 Fribourg, Switzerland

We found, in limestone Karst soils of the Jura Mountains and of the mountains in the central part of Switzerland, an enrichment up to a factor 20 of ^{230}Th and ^{226}Ra with respect to the activities of their progenitors, ^{234}U and ^{238}U . Thus, a significant radioactive disequilibrium exists between $^{238/234}\text{U}$ and ^{230}Th and ^{226}Ra . The enrichment of ^{226}Ra leads to locally high concentrations of its decay product, the noble gas ^{222}Rn . We propose continuous chemical weathering of limestone (calcite) fragments within the soil column as a plausible cause for the high ^{230}Th , ^{226}Ra , and ^{222}Rn activities. Uranium, contained within calcite, is released during weathering and migrates as stable uranyl carbonate complexes through the soil column. In contrast, its decay products (^{230}Th and ^{226}Ra) hydrolyze, are strongly sorbed to soil particles, and/or form insoluble compounds that become more and more enriched in the soil as this process continues in time.

Introduction

Unexpected high indoor radon (^{222}Rn) activities were observed at several locations in the western Jura Mountains of Switzerland (1, 2). For instance, in and around the city of La-Chaux-de-Fonds, an average of 220 Bq of $^{222}\text{Rn}/\text{m}^3$ of air was found (3) as compared to the Swiss average of 140 Bq/ m^3 (1). High indoor radon activities are of considerable concern because of the enhanced risk of lung cancer resulting from the inhalation of dust-bound α -active decay products of ^{222}Rn (4).

The Swiss watch industry in the Jura Mountains until 1965 used large quantities of ^{226}Ra , the precursor of ^{222}Rn , in luminous paints. It was, therefore, tempting to blame this industry for the enhanced radon activities of this region. Limestone, the dominant rock of the Jura Mountains, contains little ^{238}U (2–4 ppm, in agreement with ref 5) and small amounts of ^{226}Ra and is therefore generally not considered as a significant source for the release of radon. Contrary to this opinion, one of us (H.S.) and his group (2,

6, 7) found in soils at several remote locations of the Jura Mountains very high but similar enrichments in the activities of ^{230}Th and ^{226}Ra compared to the activities of their precursors ^{234}U and ^{238}U ; this means that radioactive equilibrium (i.e., equal activities and herewith an activity ratio, AR, of unity) exists between ^{230}Th and ^{226}Ra , but an expressed disequilibrium ($\text{AR} \neq 1$) has evolved between $^{234,238}\text{U}$ and ^{230}Th . Recently, we also found enrichments of ^{230}Th and ^{226}Ra in another limestone Karst region in the central Alps of Switzerland (referred to as samples from Gadmen). The following observations point strongly to a natural origin of the observed high radon activities: (i) no watch industry is or was located either at the remote locations of the Jura Mountains or in the central Alps of Switzerland; (ii) ^{230}Th was never used in luminous paints but still is highly enriched in the soils; (iii) ^{230}Th and ^{226}Ra are in radioactive equilibrium, and it is therefore very likely that ^{226}Ra resulted from the decay of ^{230}Th and not from a man-made source.

An admixture to the Jura soils of aeolian deposits (8) with high uranium contents has been given as a tentative explanation for the radioactive anomalies (7). However, the mineralogical evidence for this admixture is not quite clear. In the following, we present results of the observed anomalies, discuss a possible but more reasonable explanation than that of the presence of aeolian compounds (e.g., Loess), and propose a mechanism for the observed effects. For comparison to the limestone soils, we include investigations of non-calcite soils, namely, granite soils, and peat and Loess samples.

Radioactive disequilibrium (i.e., $\text{AR} \neq 1$ among radionuclides) in the uranium decay series is a quite common and well-investigated phenomenon that is discussed in great detail in the textbook edited by Ivanovich and Harmon (9). Very often, enrichments of ^{230}Th and ^{226}Ra were observed in the environment (10–13), but measurements of ^{230}Th and ^{226}Ra in Karst soils are scarce. The reported enrichments and related radioactive disequilibria did, to our knowledge, not nearly reach the values (reported here for the first time) of the soils of the Jura Mountains and of the central Alps of Switzerland. On the other hand, high radon values in Karst and limestone regions have been reported by others (14–16) and were attributed to residual soils concentrating uranium and radium and/or to the high permeability of karstified limestone permitting radon gas to be dispersed and transported easily. A very high radioactive disequilibrium between ^{238}U and ^{230}Th has recently been reported in a geological environment that differs very much from limestone Karst, namely, in the Western Desert of Egypt (17); here, mixing of two waters containing very different concentrations of uranium and thorium was suggested as reason for the disequilibrium. This situation is very different from that of the Jura Mountains and of the other regions in Switzerland.

Experimental Section

Figure 1 shows the sampling locations within Switzerland. The limestone Karst range of the Jura Mountains consists of Jurassic and partly Cretaceous formations with a thickness of several hundred meters. The limestone is covered by a soil layer of less than 1 m thickness. For comparison,

* Author for correspondence; telephone: +4156 310 2407; fax: +4156 310 2199.

[†] Paul Scherrer Institut.

[‡] Federal Office of Public Health.

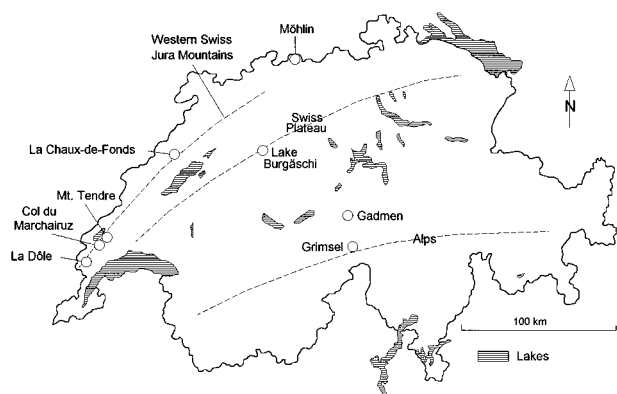


FIGURE 1. Map of Switzerland with the locations mentioned in the text, in Figure 2, and Tables 2–5. The dashed lines represent roughly the axes of geographic units, namely, the Jura Mountains, the Swiss Plateau (plains), and the Alps.

we also collected soil samples from other locations within Switzerland: (i) from a limestone formation on a slope (sampling altitude 1700 m, soil thickness ~40 cm) below the Wendenstöcke close to Gadmen (Sustenpass, central Alps); (ii) from granite soils at Handegg (Grimselpass, soil thickness ~30 cm); (iii) peat from Lake Burgäschli (Gerlafingen); and (iv) Loess from Möhlin (Aargau). These soils were formed after the last glaciation and are estimated to be $\leq 10\,000$ years old.

Most soil samples from the Jura Mountains were recovered with a soil auger from local depressions in the Karst structures. The chosen sites show in general high ^{137}Cs activities (mainly fallout from the 1986 Chernobyl release). A ^{137}Cs enrichment points to a location with an enhanced seeping of rainwater. The samples from Gadmen and Handegg were cut with a spade; great care was observed to avoid the mixing of soils from various depths. All Karst soils contained a relatively high amount of weathered limestone fragments (stones). The soils were separated by wet sieving into different fractions in the size range 100–1000 μm . Small roots were carefully separated and not used in the investigations. The peat samples were ground to a size of ~250 μm . From some soils of Mont Tendre stone fragments of several grams were recovered from the soil column during sampling. These soils also contained very small bright and black particles that were separated by hand picking.

^{238}U was determined by α -spectroscopy with surface-barrier semiconductor detectors or by the γ -rays of ^{234}Th after buildup of equilibrium between ^{234}Th and ^{238}U . Uranium-234 and ^{230}Th were measured by α -spectroscopy, and ^{226}Ra was measured by the 186 keV γ -line, corrected for contributions to this γ -line by the γ -rays of ^{235}U , taking into account the natural $^{235}\text{U}/^{238}\text{U}$ activity ratio of 0.046. For activity concentrations above 200 Bq/kg, ^{230}Th was in addition determined by its 67.5 keV γ -line, however, with a considerably larger error than in the determination by α -spectroscopy. Radon-222 was derived from the γ -activity of ^{214}Pb and ^{214}Bi , and ^{210}Pb was derived from its 46.5 keV γ -line. The γ -ray detector used is a 160 cm^3 well-type high-purity Ge detector built of low-activity materials and contained in a low-activity shielding. The maximum sample volume is 7 cm^3 . Calibration of the detector for several sample volumes has been performed with IAEA (International Atomic Energy Agency, Vienna) reference materials of comparable density and was checked by annual IAEA intercomparison exercises.

For the allocation of the ARs $^{234}\text{U}/^{238}\text{U}$ and $^{230}\text{Th}/^{234,238}\text{U}$ to specific mineral phases, several soil size fractions were further treated by sequential chemical extractions. Humic substances were extracted into 0.1 M NaOH. Amorphous iron (e.g., ferrihydrites) and/or manganese hydroxide phases were dissolved with ammonium oxalate/oxalic acid (Tamm's reagent in the dark (18)). Oxide mineral phases (e.g., goethite) were extracted with Tamm's reagent + ascorbic acid (19). The residues (mostly clay minerals and other silicates) from the previous extractions were dissolved in concentrated boiling HF/HNO₃/HClO₄. For the total samples, the ARs and uranium and thorium contents were calculated from those of the other four fractions, assuming no losses during dissolution and handling. Uranium and thorium were separated by ion exchange (20), electroplated, and measured by α -spectroscopy on semiconductor detectors. ^{232}U (in radioactive equilibrium with ^{228}Th) was used to determine the chemical yields of uranium and thorium isotopes in these separations.

The stone fragments from Mont Tendre were carefully washed with bidistilled water to remove adhering humus material. The surfaces were then etched with HCl. The cleaned stones were ground for further treatment. The resulting powder was subjected to 0.1 M NaOH to dissolve the remaining humic materials. Amorphous materials and oxides were not extracted since they are only expected at the very surfaces of the stone fragments. The stone powder was dissolved in HCl and then in HNO₃/HClO₄/HF.

The hand-picked dark and bright particles were investigated by X-ray diffraction and X-ray fluorescence. They were mainly composed of clay minerals (mostly illite), goethite, calcite, quartz, and organic materials (deduced from their sulfur content). The particles were then sequentially extracted by the usual procedures, but neglecting the humic fraction.

Results and Discussion

The radioactive decay chain of ^{238}U with the products of interest to this work is presented in Table 1. In a system closed for $> 10^6$ years (i.e., no losses or gains of any decay chain members in the investigated soil fraction during this time period), the activities of all products in the decay chain are equal (i.e., AR = 1), and one speaks of secular radioactive equilibrium between all chain members. In the natural environment, the equilibrium is often disturbed by physical and/or chemical processes (22) that enhance a loss or gain of a certain decay product.

Soils of the Jura Mountains. In Figure 2, we present the results of γ -ray measurements of ^{238}U and of a few decay products in the grain size fraction 125–250 μm of soils from Col-du-Marchairuz and from Mont Tendre. A considerable radioactive disequilibrium between ^{238}U and ^{230}Th and between ^{238}U and ^{226}Ra is observed, but radioactive equilibrium (equal activities) exists within errors between ^{230}Th and ^{226}Ra . The generally lower activity of ^{222}Rn resulted from radon losses during sample preparation and measurement; we did not attempt to re-establish, prior to measurement, radioactive equilibrium between ^{222}Rn and its precursors. The large differences between the activities of ^{226}Ra and ^{222}Rn suggest that most of the ^{226}Ra is located at the grain surfaces (a result confirmed by sequential extractions, see below), thereby allowing for an easy release of the decay product ^{222}Rn . Some of the ^{210}Pb in the top-most soil layers originated from atmospheric fallout due to decay products of ^{222}Rn . The ^{226}Ra activities

TABLE 1

Uranium-238 Decay Chain^a

Radionuclide	Half-life	Radiation
²³⁸ U	4.468 × 10 ⁹ y	α
↓		
²³⁴ Th	24.10 d	β ⁻
↓		
^{234m} , ²³⁴ Pa	1.17 min 6.70 h	β ⁻
↓		
²³⁴ U	2.446 × 10 ⁵ y	α
↓		
²³⁰ Th	7.54 × 10 ⁴ y	α
↓		
²²⁶ Ra	1600 y	α
↓		
²²² Rn	3.825 d	α
↓		
²¹⁸ Po	3.05 min	α, (β ⁻)
↓		
²¹⁴ Pb	26.8 min	β ⁻
↓		
²¹⁴ Bi	19.9 min	β ⁻ , α
↓		
²¹⁴ Po	164 μs	α
↓		
²¹⁰ Pb	22.3 y	β ⁻
↓		
²¹⁰ Bi	5.013 d	β ⁻ , (α)
↓		
²¹⁰ Po	138.38 d	α
↓		
²⁰⁶ Pb	stable	

^a The radionuclides of interest to the present work are shown in bold face letters. Decay data from Karlsruhe Nuklidkarte (27).

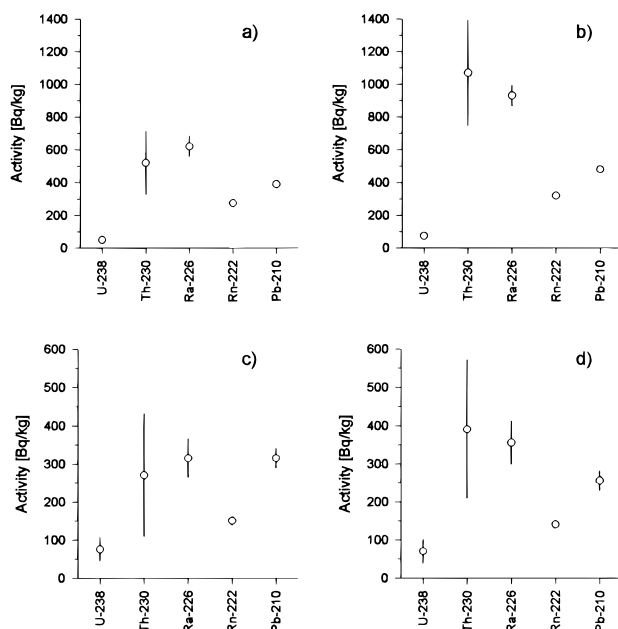


FIGURE 2. Disequilibrium in the ²³⁸U decay series in soil samples from the western Jura Mountains, Switzerland. Errors are 2σ counting errors. Grain sizes 125–250 μm. (a) and (b) Col-du-Marchairuz, 0–10 cm soil depth; (c) Mont Tendre, 0–5 cm soil depth; (d) Mont Tendre, 5–10 cm soil depth.

are up to 30 times higher than average values for Swiss Plateau soils (23). Radon, emanating from the ²²⁶Ra accumulations, can be transported by soil water into cavities of the Karst system from where it diffuses into houses (24). High radon activities in soils of Karst regions were also observed by others (e.g., refs 15 and 16).

To obtain information on the distribution of radionuclides among several soil phases and minerals, standard sequential chemical extractions (18, 19) were performed. It must, however, be pointed out that chemical extractions are always operational procedures. Therefore, the extracted phases may vary considerably from sample to sample, and the indicated compositions of the soils are only crude approximations.

In Tables 2–4, we show the results of samples from Col-du-Marchairuz and from Mont Tendre that were treated by sequential chemical extractions. In the following sections, we discuss separately the ²³⁴U/²³⁸U and ²³⁰Th/²³⁴U ARs and the uranium and thorium concentrations presented in these tables.

²³⁴U/²³⁸U Activity Ratios. The ARs ²³⁴U/²³⁸U are generally somewhat higher than unity in the humic and amorphous materials and oxides of the samples from Col-du-Marchairuz (Table 2) and from Mont Tendre (Table 3), but are smaller than unity in the residues remaining from the sequential extractions. These residues represent inert bulk soil grains that can only be dissolved by strong acids. The ARs (> 1) of the humic substances and the amorphous and oxide phases result from surface sorption of uranium by these materials from the interstitial soil water, which usually has ²³⁴U/²³⁸U ARs of > 1 (22). The slight enrichment of ²³⁴U relative to ²³⁸U in the interstitial soil water results from recoil processes in the solid phases related to α-decay (25). Contrary, in the residues and in the total samples (calculated from the other four fractions) these ratios are predominantly < 1 due to preferential losses of ²³⁴U from the solid materials to the soil solution by the α-recoil processes discussed in ref 22.

²³⁰Th/²³⁴U Activity Ratios. Contrary to ²³⁴U/²³⁸U, the ARs ²³⁰Th/²³⁴U of the humic materials and the amorphous and oxide phases from Col-du-Marchairuz (Table 2) and Mont Tendre (Table 3) are much higher than unity. The highest ARs (4.6–18.7) were found in the humic and amorphous materials. In the oxides, they were 1.5–10.4. The high ARs of ²³⁰Th/²³⁴U are due to a preferential accumulation of ²³⁰Th in the soils. The accumulation is caused by hydrolyzed and insoluble thorium compounds that are more firmly bound to soil particles than uranium complexes. The sequential extractions primarily affect grain surfaces and surface-related materials. Therefore, our observations point to significant enrichments of ²³⁰Th (and ²²⁶Ra, see Figure 2) on soil grain surfaces. This is in agreement with refs 26–29, which have pointed out that the radioactive decay products accumulate preferentially in thin grain surface layers consisting of hydroxides, oxides, or organic deposits. ²²²Rn emanates easily and almost quantitatively from such thin layers of surface deposits. This was confirmed in our laboratory experiments (see above).

In the residues, the ARs of ²³⁰Th/²³⁴U are < 1 (with three exceptions). The small ARs in these materials are probably also a result of physical and chemical changes produced by α-recoil, but they are not fully understood. The enrichment of ²³⁰Th is still discernible in the total samples (calculated from the other four phases), but the effects are reduced by the large contributions of the residues, which represent weight-wise the most important fractions. Unfortunately, none of the investigated soil fractions is truly a closed system that could be used to estimate a soil age from the disequilibrium between ²³⁰Th and ^{234,238}U.

TABLE 2

Activity Ratios $^{234}\text{U}/^{238}\text{U}$ and $^{230}\text{Th}/^{234}\text{U}$ (with 1σ Counting Errors) and Concentrations of Uranium and Thorium in Samples from Col-du-Marchairuz (Jura Mountains)^a

activity ratio	samples (depth below surface)					
	0–5 cm	5–10 cm	10–20 cm	20–30 cm	30–40 cm	0–20 cm
Humic Materials						
$^{234}\text{U}/^{238}\text{U}$	1.00 ± 0.03	1.04 ± 0.03	1.09 ± 0.04	1.19 ± 0.05	1.09 ± 0.03	1.03 ± 0.06
$^{230}\text{Th}/^{234}\text{U}$	9.71 ± 0.10	10.67 ± 0.19	11.84 ± 0.19	12.07 ± 0.33	13.76 ± 0.10	16.00 ± 0.18
^{238}U (μg/g of sample)	1.17	1.06	0.91	0.76	0.77	0.58
^{232}Th (μg/g of sample)	1.75	1.91	1.94	1.83	1.61	0.92
Amorphous Materials						
$^{234}\text{U}/^{238}\text{U}$	1.08 ± 0.04	1.11 ± 0.03	1.05 ± 0.03	1.07 ± 0.03	1.04 ± 0.02	1.09 ± 0.04
$^{230}\text{Th}/^{234}\text{U}$	6.00 ± 0.22	4.59 ± 0.14	5.58 ± 0.13	6.00 ± 0.12	6.17 ± 0.09	10.62 ± 0.16
^{238}U (μg/g of sample)	0.59	1.31	1.06	1.24	1.55	0.82
^{232}Th (μg/g of sample)	0.68	1.1	1.02	1.32	1.77	0.95
Oxides						
$^{234}\text{U}/^{238}\text{U}$	0.97 ± 0.04	0.87 ± 0.04	0.93 ± 0.04	1.01 ± 0.04	0.95 ± 0.04	1.35 ± 0.09
$^{230}\text{Th}/^{234}\text{U}$	2.81 ± 0.08	4.72 ± 0.15	3.39 ± 0.12	3.97 ± 0.14	5.28 ± 0.21	1.48 ± 0.38
^{238}U (μg/g of sample)	0.36	0.4	0.43	0.41	0.5	0.20
^{232}Th (μg/g of sample)	0.62	0.68	0.67	0.69	0.88	0.62
Residue						
$^{234}\text{U}/^{238}\text{U}$	0.60 ± 0.01	0.60 ± 0.01	0.60 ± 0.01	0.62 ± 0.01	0.62 ± 0.01	0.87 ± 0.03
$^{230}\text{Th}/^{234}\text{U}$	0.57 ± 0.01	0.86 ± 0.01	0.67 ± 0.01	0.71 ± 0.01	0.79 ± 0.01	7.21 ± 0.11
^{238}U (μg/g of sample)	5.02	3.24	6.24	6.35	6.36	0.89
^{232}Th (μg/g of sample)	2.63	3.97	3.60	3.76	3.64	2.12
Total Sample^b						
$^{234}\text{U}/^{238}\text{U}$	0.72	0.62	0.72	0.75	0.75	1.02
$^{230}\text{Th}/^{234}\text{U}$	2.63	3.66	2.58	2.59	3.03	11.06
^{238}U (μg/g of sample)	7.14	6.01	8.64	8.76	9.18	2.5
^{232}Th (μg/g of sample)	5.68	7.66	7.23	7.6	7.9	4.61

^a Grain size for all samples is <1 mm. ^b Calculated from the other four fractions, assuming no losses in handling.

TABLE 3

Activity Ratios of $^{234}\text{U}/^{238}\text{U}$ and $^{230}\text{Th}/^{234}\text{U}$ (with 1σ Counting Errors) and Concentrations of Uranium and Thorium in Samples from Mont Tendre (Jura Mountains)^a

activity ratio	samples (depth)				
	1 (0–5 cm)	2 (5–10 cm)	3 (0–20 cm)	4 (20–40 cm)	5 (40–50 cm)
Humic Materials					
$^{234}\text{U}/^{238}\text{U}$	1.14 ± 0.06	1.03 ± 0.05	1.17 ± 0.11	1.16 ± 0.14	1.20 ± 0.16
$^{230}\text{Th}/^{234}\text{U}$	12.88 ± 0.25	13.06 ± 0.12	18.17 ± 0.42	14.14 ± 0.45	5.88 ± 0.24
^{238}U (μg/g of sample)	0.46	0.58	0.13	0.06	0.05
^{232}Th (μg/g of sample)	1.92	2.06	1.01	0.27	0.13
Amorphous Materials					
$^{234}\text{U}/^{238}\text{U}$	1.39 ± 0.12	2.26 ± 0.12	1.05 ± 0.08	1.04 ± 0.08	1.25 ± 0.11
$^{230}\text{Th}/^{234}\text{U}$	14.00 ± 0.58	12.03 ± 0.56	18.37 ± 0.68	7.10 ± 0.53	5.42 ± 0.32
^{238}U (μg/g of sample)	0.29	0.32	0.24	0.26	0.13
^{232}Th (μg/g of sample)	1.55	2.47	1.89	0.82	0.38
Oxides					
$^{234}\text{U}/^{238}\text{U}$	1.17 ± 0.10	1.04 ± 0.07	0.97 ± 0.10	1.33 ± 0.14	1.23 ± 0.16
$^{230}\text{Th}/^{234}\text{U}$	4.15 ± 0.42	4.20 ± 0.20	10.42 ± 0.45	9.39 ± 0.73	5.47 ± 0.46
^{238}U (μg/g of sample)	0.23	0.28	0.13	0.10	0.10
^{232}Th (μg/g of sample)	1.13	1.08	0.89	0.63	0.38
Residues					
$^{234}\text{U}/^{238}\text{U}$	0.69 ± 0.01	0.69 ± 0.01	0.73 ± 0.02	0.72 ± 0.02	0.80 ± 0.03
$^{230}\text{Th}/^{234}\text{U}$	0.70 ± 0.02	0.62 ± 0.01	lost ^c	1.84 ± 0.04	2.09 ± 0.06
^{238}U (μg/g of sample)	3.62	4.00	2.95	2.44	1.27
^{232}Th (μg/g of sample)	3.33	3.58	lost ^c	4.38	2.46
Total Sample^b					
$^{234}\text{U}/^{238}\text{U}$	0.80	0.84	0.77	0.78	0.87
$^{230}\text{Th}/^{234}\text{U}$	2.93	2.91	lost ^c	2.84	2.71
^{238}U (μg/g of sample)	4.60	5.17	3.45	2.86	1.55
^{232}Th (μg/g of sample)	7.93	9.19	lost ^c	6.1	3.55

^a Samples 1 and 2, grain size 125–250 μm; samples 3–5, grain size <250 μm. Samples 1 and 2 are from slightly different locations, samples 3 to 5 from different depths at location 2. ^b Calculated from the other four fractions, assuming no losses in handling. ^c Lost during chemical treatment.

Uranium and Thorium Concentrations. In Tables 2 and 3, we also show the uranium and thorium concentra-

tions of the investigated mineral phases. The indicated concentrations are given for 1 g of total sample and not for

TABLE 4

Activity Ratios of $^{234}\text{U}/^{238}\text{U}$ and $^{230}\text{Th}/^{234}\text{U}$ (with 1σ Counting Errors) and Uranium and Thorium Concentrations in Samples from Mont Tendre^a

activity ratio	1st stone	2nd stone	dark particles	bright particles
		Humic Materials		
$^{234}\text{U}/^{238}\text{U}$	1.14 ± 0.03	1.06 ± 0.04	nd ^c	nd ^c
$^{230}\text{Th}/^{234}\text{U}$	0.85 ± 0.02	0.86 ± 0.03	nd	nd
^{238}U (μg/g of sample)	0.44	0.44	nd	nd
^{232}Th (μg/g of sample)	0.24	0.23	nd	nd
		Amorphous Materials		
$^{234}\text{U}/^{238}\text{U}$	nd ^c	nd ^c	1.03 ± 0.03	1.14 ± 0.06
$^{230}\text{Th}/^{234}\text{U}$	nd	nd	14.84 ± 0.06	20.34 ± 0.74
^{238}U (μg/g of sample)	nd	nd	2.31	0.46
^{232}Th (μg/g of sample)	nd	nd	lost ^d	lost ^d
		Oxides		
$^{234}\text{U}/^{238}\text{U}$	nd ^c	nd ^c	1.29 ± 0.16	1.39 ± 0.19
$^{230}\text{Th}/^{234}\text{U}$	nd	nd	18.06 ± 0.87	5.59 ± 0.28
^{238}U (μg/g of sample)	nd	nd	0.32	0.30
^{232}Th (μg/g of sample)	nd	nd	lost ^d	lost ^d
		Residues		
$^{234}\text{U}/^{238}\text{U}$	0.74 ± 0.02	0.73 ± 0.02	0.75 ± 0.02	0.99 ± 0.05
$^{230}\text{Th}/^{234}\text{U}$	1.00 ± 0.03	1.12 ± 0.04	8.17 ± 0.14	3.50 ± 0.19
^{238}U (μg/g of sample)	3.54	3.92	1.85	1.00
^{232}Th (μg/g of sample)	0.65	0.54	nd	nd
		Total Samples ^b		
$^{234}\text{U}/^{238}\text{U}$	nd ^c	nd ^c	0.93	1.10
$^{230}\text{Th}/^{234}\text{U}$	nd	nd	12.31	8.26
^{238}U (μg/g of sample)	3.89	4.36	4.48	1.76
^{232}Th (μg/g of sample)	0.89	0.77	lost ^d	lost ^d

^a Fragments of calcite stones (about 20 g) and hand-picked particles, size ~1 mm (see text). ^b Calculated from the other four fractions, assuming no losses in handling. ^c nd, not detected. ^d Lost during chemical treatment.

1 g of the respective mineral phases. It is obvious that the residues contain by far the largest quantities of ^{238}U and ^{232}Th . The measured uranium concentrations of the residues and total samples are higher than those normally observed in limestones and point to an enrichment of uranium in certain phases of these soils.

Stones and Selected Soil Particles. In Table 4, we compare fragments of calcite stones and striking dark and bright particles that were recovered from the soil column of Mont Tendre.

Stones. The $^{230}\text{Th}/^{234}\text{U}$ ARs of the humic materials within the matrix of the two stones differ very much from those of soil samples from Mont Tendre. In contrast to the soils, ^{230}Th is depleted in these humic materials relative to ^{234}U . This indicates a transfer of ^{230}Th by α -recoil from the humic materials into the solid stone matrix. The concentrations of ^{232}Th are low compared with the humic materials of the soil samples.

Only negligible activities were detected in the solutions resulting from HCl extractions of the stones. This shows that the calcite phase does not contain many impurities. Uranium and thorium and their decay products were almost completely contained in the residues (e.g., in clay minerals or other silicates). Here, the $^{234}\text{U}/^{238}\text{U}$ ARs are <1, demonstrating enhanced weathering of ^{234}U due to α -recoil combined with a subsequent mobilization of this uranium isotope. On the other hand, the $^{230}\text{Th}/^{234}\text{U}$ ARs are unity, or somewhat larger than 1, supporting the assumption of an enrichment of ^{230}Th due to α -recoil processes and demonstrating the immobility of thorium compounds.

Particles. In the dark and bright particles, the $^{234}\text{U}/^{238}\text{U}$ ARs are close to unity in all fractions (no extraction of humic materials). This contrasts again to the $^{230}\text{Th}/^{234}\text{U}$ ARs that have high values in all fractions, including the

residues. The high ARs may be caused by strong sorption of thorium to clay minerals, iron compounds (e.g., goethite), and organic materials that are enriched in these particles, as demonstrated by the X-ray investigations.

Comparison of Various Soils. In Table 5, we present the mean results (and their 1σ standard deviations) of the analyses of all soil samples and mineral fractions from 16 Karst soils of the Jura Mountains and two soils from Gadmen and compare them with those obtained in Loess and peat samples and in two granite soils. The ARs of $^{234}\text{U}/^{238}\text{U}$ are similar in all samples and mineral phases, are mostly somewhat larger than unity, and reflect the isotopic composition of uranium in the soil solutions from where it is sorbed to grain surfaces (26–29). This contrasts sharply with the ARs of $^{230}\text{Th}/^{234}\text{U}$. These latter exhibit very high values in the humic, amorphous, and oxidic soil fractions of the Jura Mountains and in the soils recovered close to Gadmen, demonstrating the importance of thorium sorption to these phases. The $^{230}\text{Th}/^{234}\text{U}$ ARs of the Karst regions differ considerably from the ARs of the Loess, peat, and granite samples. The latter ARs are much smaller, sometimes even <1. Possible reasons for these differences are discussed below. The differences in the ARs between limestone soils and Loess also question the early hypothesis (7) of an admixture of aeolian compounds to Jura soils (8) as an explanation of the radioactive anomalies (see Introduction to this paper).

The observed large radioactive disequilibrium between $^{234,238}\text{U}$ and ^{230}Th in most of the investigated soils and phases from the limestone Karst regions of the Jura Mountains and from Gadmen is the result of chemical fractionation of uranium and thorium (22). Uranium is expected to exist in the interstitial waters of these calcite soils in the form of very stable, anionic [e.g., $\text{UO}_2(\text{CO}_3)_3^{4-}$], or neutral

TABLE 5

Comparison of Activity Ratios of $^{234}\text{U}/^{238}\text{U}$ and $^{230}\text{Th}/^{234}\text{U}$ and Uranium and Thorium Concentrations with Standard Deviations (1σ) in Limestone Soils from the Jura Mountains and from Gadmen with Those of Loess, Peat, and Granite Soils

activity ratio	Jura (mean) ($n = 16$) ^a	Gadmen (mean) ($n = 2$) ^a	Loess Mhlin ($n = 1$) ^a	peat ($n = 1$) ^a	granite soil (mean) ($n = 2$) ^a
Humic Materials					
$^{234}\text{U}/^{238}\text{U}$	1.10 ± 0.08	1.20 ± 0.21	1.35	1.26	1.05 ± 0.02
$^{230}\text{Th}/^{234}\text{U}$	12.08 ± 3.49	4.97 ± 1.32	0.99	0.34	0.12 ± 0.01
^{238}U ($\mu\text{g/g}$ of sample)	0.58 ± 0.38	0.27 ± 0.03	0.11	0.29	2.65 ± 0.51
^{232}Th ($\mu\text{g/g}$ of sample)	1.33 ± 0.71	1.11 ± 0.02	0.34	0.24	0.69
Amorphous Materials					
$^{234}\text{U}/^{238}\text{U}$	1.21 ± 0.35	1.25 ± 0.06	2.28	1.26	1.04 ± 0.02
$^{230}\text{Th}/^{234}\text{U}$	8.57 ± 4.60	5.71 ± 0.13	10.39	0.82	2.83 ± 0.11
^{238}U ($\mu\text{g/g}$ of sample)	0.66 ± 0.41	0.28 ± 0.01	0.03	0.07	0.97 ± 0.23
^{232}Th ($\mu\text{g/g}$ of sample)	1.36 ± 0.81	1.65 ± 0.12	1.81	0.18	5.68 ± 1.42
Oxides					
$^{234}\text{U}/^{238}\text{U}$	1.12 ± 0.23	1.03 ± 0.17	1.00	1.09	1.05 ± 0.07
$^{230}\text{Th}/^{234}\text{U}$	6.81 ± 4.58	3.22 ± 0.62	3.12	2.77	1.17 ± 0.04
^{238}U ($\mu\text{g/g}$ of sample)	0.25 ± 0.12	0.17 ± 0.01	0.10	0.04	0.85 ± 0.05
^{232}Th ($\mu\text{g/g}$ of sample)	0.78 ± 0.29	0.88	1.14	0.24	2.70 ± 0.28
Residues					
$^{234}\text{U}/^{238}\text{U}$	0.71 ± 0.10	0.92 ± 0.02	1.04	1.23	1.05 ± 0.02
$^{230}\text{Th}/^{234}\text{U}$	2.23 ± 2.53	0.82 ± 0.16	0.78	1.23	0.62 ^c
^{238}U ($\mu\text{g/g}$ of sample)	3.22 ± 1.91	1.71 ± 0.05	1.60	0.11	1.83 ± 0.14
^{232}Th ($\mu\text{g/g}$ of sample)	3.37 ± 0.95	3.97 ± 1.24	4.64	0.29	1.96 ± 0.02
Total Samples ^b					
$^{234}\text{U}/^{238}\text{U}$	0.82 ± 0.12	0.99 ± 0.01	1.07	1.25	1.05 ± 0.02
$^{230}\text{Th}/^{234}\text{U}$	4.29 ± 3.36	2.00	1.08	0.79	0.84
^{238}U ($\mu\text{g/g}$ of sample)	4.66 ± 2.49	2.42 ± 0.06	1.84	0.51	6.30 ± 0.54
^{232}Th ($\mu\text{g/g}$ of sample)	6.70 ± 2.01	7.60 ± 1.10	7.93	0.95	11.84

^a Number of investigated soil samples. ^b Calculated from the other four fractions, assuming no losses in handling. ^c One sample lost during chemical treatment.

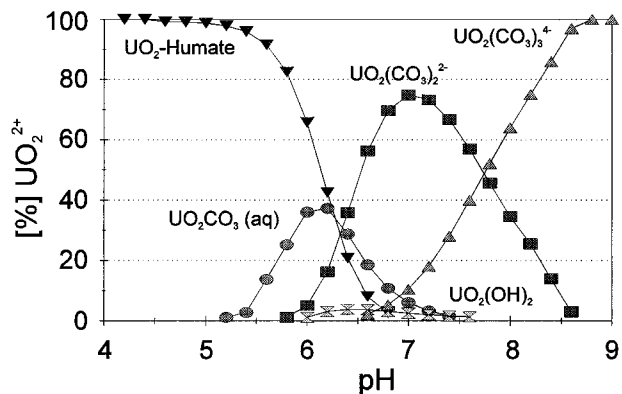


FIGURE 3. Calculated speciation of uranium in groundwater. The program MINTQA2 (37) and formation constants of NEA (38), of ref 39, and from the data base of Paul Scherrer Institut were used (30).

carbonate complexes, as shown in Figure 3. These complexes are very mobile and/or only slightly or not at all sorbed by negatively charged soil surfaces (30). On the other hand, thorium hydrolyses very easily (32, 33) and is strongly and rapidly adsorbed by soil surfaces (34). At pH values > 7, it sorbs almost completely onto clay minerals or organic matter (32). Therefore, it accumulates along the soil column. The pH (~7–8) and the alkalinity (~5 mM) of these soils are not high enough for a significant dissolution of thorium due to complexation by carbonates (35, 36). The soil is old enough ($\leq 10\,000$ years, i.e., formed after the end of the last glaciation) to establish radioactive equilibrium between ^{230}Th and ^{226}Ra . In agreement with our results, a preferential migration of uranium as compared to thorium has also been described for soils in Syria (37).

In contrast to the results of the Karst soils, the investigated granite soils and the peat and Loess samples suggest a relatively similar behavior of both uranium and thorium in these materials. In the absence of high CO_2 concentrations produced by calcite weathering that enhance the formation of stable and soluble uranium carbonate complexes, uranium may form insoluble complexes, e.g., with humic substances (30), and thus be less mobile than in the slightly alkaline calcite (limestone) soils. The more acidic granite soils may enhance the formation of humic complexes as shown in Figure 3.

The high ^{230}Th and ^{226}Ra enrichments in Karst soils can be explained by a steady dissolution of the abundant limestone (calcite) fragments within the soil column. The uranium concentrations in limestone pieces from Mont Tendre soils amounted to $\sim 4\ \mu\text{g/g}$ (Table 4). With this uranium concentration and a relatively homogeneous distribution of the limestone fragments throughout the soil column, a few 10 g of dissolved fragments/g of present-day soil would be sufficient to produce the observed activities of ^{230}Th and ^{226}Ra . Within the time frame available (i.e., $\gg 1000$ years), even a very slow dissolution of limestone would be sufficient to account for the observed effects. Furthermore, the dissolution of limestone within soils is enhanced by the higher CO_2 partial pressure ($\geq 10^{-2}$ atm) from bacteria-mediated decomposition of organic matter. However, the hypothesis of a limestone source of uranium that could produce the high enrichments of ^{230}Th and ^{226}Ra and eventually the high indoor ^{222}Rn concentrations needs to be investigated further.

We expect that high ^{230}Th and ^{226}Ra enrichments and, consequently, high indoor ^{222}Rn concentrations also prevail in other limestone Karst regions. Therefore, we strongly

suggest that similar studies should be carried out in Karst regions around the world.

Conclusions

Very high activity ratios of $^{230}\text{Th}/^{234}\text{U}$ are observed in limestone Karst regions of Switzerland. The high enrichments of ^{230}Th (and ^{226}Ra) are mainly found in surface-related fractions of humic, amorphous (e.g., ferrihydrites), and oxidic (e.g., goethite) materials.

The presented results support a natural origin of the exceptionally high concentrations of ^{230}Th , ^{226}Ra , and ^{222}Rn in limestone Karst soils.

The high concentrations of ^{230}Th and ^{226}Ra and the related radioactive disequilibrium between $^{234,238}\text{U}$ and ^{230}Th and ^{226}Ra are very likely produced by the weathering of calcite, hereby releasing uranium and its decay products.

Uranium migrates as a stable (carbonate) complex and leaves ^{230}Th in the soil. The latter accumulates steadily, and ^{226}Ra grows in and finally reaches radioactive equilibrium with ^{230}Th .

Non-Karstic soils do not exhibit the very large radioactive disequilibria of the uranium decay series.

Acknowledgments

We thank U. Krähenbühl and E. Hoehn for discussions, M. Bradbury for stylistic improvements, and R. Keil for analytical help. R. Giovanoli performed the X-ray analyses. We thank the two anonymous reviewers for their constructive remarks.

Literature Cited

- (1) 30. Bericht Eidgenössische Kommission zur Überwachung der Radioaktivität: 1987/88; Eidgenössische Drucksachen und Materialzentrale: Bern, Switzerland, 1991.
- (2) Surbeck, H. *Radiat. Prot. Dosim.* **1988**, *24*, 431–434.
- (3) Lauffenburger, T.; Auf der Maur, A. *Proc. 6th Int. Congr. IRPA*, **1984**.
- (4) Protection Against Radon-222 at Home and Work. ICRP Publication 65; *Ann. ICRP* **1993**, *23/2*.
- (5) Gascoyne, M. In *Uranium-Series Disequilibrium*, 2nd ed.; Ivanovich, M., Harmon, R. S., Eds.; Clarendon Press: Oxford, 1992; pp 34–61.
- (6) Surbeck, H.; Piller, G. *Proceedings of the 1988 International Symposium on Radon/Radon Reduction Technology*; EPA-600/9-89-006; U.S. EPA: Washington, DC, 1989.
- (7) Surbeck, H. *Proceedings of the 1992 International Symposium on Radon and Radon Reduction Technology*; EPA-600/R-93-0836; U.S. EPA: Washington, DC, 1992.
- (8) Pochon, M. *Mem. Soc. Helv. Sci. Nat.* **1978**, *90*.
- (9) Ivanovich, M.; Harmon, R. S. *Uranium-Series Disequilibrium*, 2nd ed.; Clarendon Press: Oxford, 1992.
- (10) Titayeva, N. A.; Veksler, T. I. *Geochem. Int.* **1977**, *14*, 99–107.
- (11) Airey, P. L.; Roman, D. J. *Geol. Soc. Aust.* **1981**, *28*, 357–363.
- (12) Latham, A. G.; Schwarcz, H. P. *Geochim. Cosmochim. Acta* **1987**, *51*, 2787–2793.
- (13) Ivanovich, M.; Latham, A. G.; Longworth, G.; Gascoyne, M. In *Uranium-Series Disequilibrium*, 2nd ed.; Ivanovich, M., Harmon, R. S., Eds.; Clarendon Press: Oxford, 1992; pp 583–630.
- (14) Damkjær, A.; Korsbech, U. *Radiat. Prot. Dosim.* **1988**, *24*, 51–54.
- (15) Ball, T. K.; Cameron, D. G.; Colman, T. B. *Radiat. Prot. Dosim.* **1992**, *45*, 2122–214.
- (16) Ball, T. K.; Miles, J. C. H. *Environ. Geochem. Health* **1993**, *15*, 27–35.
- (17) Dabous, A. A. *Geochim. Cosmochim. Acta* **1994**, *58*, 4591–4600.
- (18) Schwertmann, U. *Clay Miner.* **1984**, *19*, 9–19.
- (19) Shuman, L. M. *Soil Sci.* **1985**, *140*, 11–22.
- (20) Gindler, J. E. *The Radiochemistry of Uranium*; NAS-NS 3050; U.S. Atomic Energy Commission: Washington, DC, 1962.
- (21) *Karlsruher Nuklidkarte*, 5; Kernforschungszentrum: Karlsruhe, Germany; 1981.
- (22) Osmond, J. K.; Ivanovich, M. In *Uranium-Series Disequilibrium*, 2nd ed.; Ivanovich, M., Harmon, R. S., Eds.; Clarendon Press: Oxford, 1992; pp 259–289.
- (23) Surbeck, H.; Völkle, H.; Zeller, W. *Proceedings of the 1991 International Symposium on Radon and Radon Reduction Technology*; EPA-600/9-91-37a-d; U.S. EPA: Washington, DC, 1992.
- (24) Surbeck, H.; Medici, F. *Hydrology in Mountainous Regions: Proceedings of the International Conference on Water Resources in Mountainous Regions*, Lausanne, Switzerland, 1990; International Association of Hydrological Sciences: Wallingford, 1990; IAHS-AISH Publication 193-194.
- (25) Fleischer, R. L. *Geochim. Cosmochim. Acta* **1982**, *46*, 2191–2291.
- (26) Gascoyne, M.; Cramer, J. J. *Appl. Geochem.* **1987**, *2*, 37–54.
- (27) Longworth, G.; Ivanovich, M.; Hasler, S. A. Measurements of the partition of long-lived uranium and thorium isotopes in mineral phases of Eden Shale (Lounthwaite) and granite (Strath Halladale). Nirex Report NSS/R181, 1989.
- (28) Dearlove, J. P. L.; Green, D. C.; Ivanovich, M. *Proc. Mat. Res. Soc. Symp.* **1989**, *127*, 927–932.
- (29) Dearlove, J. P. L.; Ivanovich, M.; Green, D. C. In *Proceedings of the 6th Water/Rock Interaction Symposium*, Malvern, U.K.; Balkema: Rotterdam, 1990; pp 191–195.
- (30) Lienert, Ch.; Short, S. A.; von Gunten, H. R. *Geochim. Cosmochim. Acta* **1994**, *58*, 5455–5463.
- (31) Allison, J. D.; Brown, D. S.; Novo-Gradac, K. J. *MINTEQA2/PRODEFA2, a Geochemical Assessment Model for Environmental Systems: Version 3.0*; U.S. Environmental Protection Agency: Athens, GA, 1991.
- (32) Langmuir, D.; Herman, J. S. *Geochim. Cosmochim. Acta* **1980**, *44*, 1753–1766.
- (33) Clark, D. L.; Hobart, D. E.; Neu, M. P. *Chem. Rev.* **1995**, *95*, 25–48.
- (34) Krishnaswami, S.; Graustein, W. C.; Turekian, K. K. *Water Resour. Res.* **1982**, *18*, 1633–1675.
- (35) LaFlamme, B. D.; Murray, J. W. *Geochim. Cosmochim. Acta* **1987**, *51*, 243–250.
- (36) Östholts, E.; Bruno, J.; Grenthe, I. *Geochim. Cosmochim. Acta* **1994**, *58*, 613–623.
- (37) Hillaire-Marcel, C.; Vallières, S.; Ghaleb, B.; Mareschal, J. C. *Comptes Rendus, Ser. 2*, **1990**, *311*, 233–238.
- (38) *Predicted Formation Constants Using the Unified Theory of Metal Ion Complexation*; Nuclear Energy Agency, OECD/NEA: Paris, 1987.
- (39) Choppin, G. R.; Allard, B. In *Handbook on the Physics and Chemistry of Actinides Vol. 3*; Freeman, A. J., Keller, C., Eds.; Elsevier: Amsterdam, 1985; pp 407–429.

Received for review July 3, 1995. Revised manuscript received November 3, 1995. Accepted November 6, 1995.[®]

ES950473J

[®] Abstract published in *Advance ACS Abstracts*, February 1, 1996.